symmetry

Article

Underground Tests of Quantum Mechanics by the VIP Collaboration at Gran Sasso

Fabrizio Napolitano [1,*], Andrea Addazi [1,2], Angelo Bassi [3,4], Massimiliano Bazzi [1], Mario Bragadireanu [1,5], Michael Cargnelli [6], Alberto Clozza [1], Luca De Paolis [1], Raffaele Del Grande [1,7], Maaneli Derakhshani [8], Sandro Donadi [4], Carlo Fiorini [9], Carlo Guaraldo [1], Mihail Iliescu [1], Matthias Laubenstein [10], Simone Manti [1], Antonino Marcianò [1,11], Johann Marton [1,6], Marco Miliucci [1], Edoardo Milotti [3,4], Kristian Piscicchia [1,12], Alessio Porcelli [1,12], Alessandro Scordo [1], Francesco Sgaramella [1], Diana Laura Sirghi [1,5,12], Florin Sirghi [1,5], Oton Vazquez Doce [1], Johann Zmeskal [1,6] and Catalina Curceanu [1,5]

1. INFN, Laboratori Nazionali di Frascati, Via E. Fermi 54, I-00044 Roma, Italy
2. Center for Theoretical Physics, College of Physics Science and Technology, Sichuan University, Chengdu 610065, China
3. Dipartimento di Fisica, Università di Trieste, Strada Costiera 11, 34151 Miramare-Trieste, Italy
4. INFN-Sezione di Trieste, Via Valerio 2, I-34127 Trieste, Italy
5. IFIN-HH, Institutul National pentru Fizica si Inginerie Nucleara Horia Hulubei, Str. Atomistilor No. 407, P.O. Box MG-6 Bucharest-Magurele, Romania
6. Stefan-Meyer-Institute for Subatomic Physics, Austrian Academy of Science, Kegelgasse 27, 1030 Vienna, Austria
7. Physik Department E62, Technische Universität München, James-Franck-Straße 1, D-85748 Garching, Germany
8. Departement of Mathematics, Rutgers University, New Brunswick, NJ 08854-8019, USA
9. Politecnico di Milano, Dipartimento di Elettronica, Informazione e Bioingegneria and INFN Sezione di Milano, I-20133 Milano, Italy
10. Laboratori Nazionali del Gran Sasso, INFN, Via G. Acitelli 22, I-67100 L'Aquila, Italy
11. Department of Physics, Fudan University, (Jiangwan Campus) Office n S234, 2005 Songhu Road, Shanghai 200438, China
12. Centro Ricerche Enrico Fermi–Museo Storico della Fisica e Centro Studi e Ricerche "Enrico Fermi", Via Panisperna 89a, I-00184 Roma, Italy

* Correspondence: fabrizio.napolitano@lnf.infn.it; Tel.: +39-06-940-31-2569

Citation: Napolitano, F.; Addazi, A.; Bassi, A.; Bazzi, M.; Bragadireanu, M.; Cargnelli, M.; Clozza, A.; De Paolis, L.; Del Grande, R.; Derakhshani, M.; et al. Underground Tests of Quantum Mechanics by the VIP Collaboration at Gran Sasso. *Symmetry* **2023**, *15*, 480. https://doi.org/10.3390/sym15020480

Academic Editors: Ilya G. Kaplan and Manuel Gadella

Received: 23 December 2022
Revised: 17 January 2023
Accepted: 3 February 2023
Published: 11 February 2023

Abstract: Modern physics lays its foundations on the pillars of Quantum Mechanics (QM), which has been proven successful to describe the microscopic world of atoms and particles, leading to the construction of the Standard Model. Despite the big success, the old open questions at its very heart, such as the measurement problem and the wave function collapse, are still open. Various theories consider scenarios which could encompass a departure from the predictions of the standard QM, such as extra-dimensions or deformations of the Lorentz/Poincaré symmetries. At the Italian National Gran Sasso underground Laboratory LNGS, we search for evidence of new physics proceeding from models beyond standard QM, using radiation detectors. Collapse models addressing the foundations of QM, such as the gravity-related Diósi–Penrose (DP) and Continuous Spontaneous Localization (CSL) models, predict the emission of spontaneous radiation, which allows experimental tests. Using a high-purity Germanium detector, we could exclude the natural parameterless version of the DP model and put strict bounds on the CSL one. In addition, forbidden atomic transitions could prove a possible violation of the Pauli Exclusion Principle (PEP) in open and closed systems. The VIP-2 experiment is currently in operation, aiming at detecting PEP-violating signals in Copper with electrons; the VIP-3 experiment upgrade is foreseen to become operative in the next few years. We discuss the VIP-Lead experiment on closed systems, and the strong bounds it sets on classes of non-commutative quantum gravity theories, such as the θ–Poincaré theory.

Keywords: wavefunction collapse; Pauli exclusion principle; X-rays; VIP-2; fundamental symmetries

1. Introduction

QM successfully accounts for observations of microscopic phenomena since its formulation about a hundred years ago; its subsequent relativistic field formulation is the building ground of the Standard Model (SM), extending quantum dynamics to the electromagnetic, weak and strong interactions. Despite the great scientific effort devoted to investigating the SM validity, there are a few shortcomings, both experimentally and theoretically. Neutrino masses, matter–antimatter asymmetry, dark matter and dark energy are a few examples. Incorporating gravity into the SM poses the biggest theoretical challenge. Precision tests involve quantum mechanics under two different perspectives.

A first approach, which we call *bottom-up*, originates from the main question that remains unanswered in quantum theory and may point the way to a better understanding of Nature's laws: the measurement problem and the wave function collapse. The debate around the wave function collapse sparked when Schrödinger presented his famous cat paradox [1]. In the Schrödinger equation, microscopic objects exist in a superposition of states and evolve in time linearly and deterministically. The description of the quantum objects changes with the wave function reduction postulate, where the evolution is instead nonlinear and stochastic. While the reduction postulate successfully explains the outcome of the experiments, it still appears like an ad hoc artifice, missing a more fundamental origin. In order to explain the wave function collapse, accounting for the lack of superposition in macroscopic objects, a breakdown of the linear, deterministic evolution was proposed [2–7].

Penrose and Diósi (DP) formulated, independently, an approach where the gravitational self-potential impacts the dynamics of the collapse [8–12]. A characteristic time of collapse τ_{DP} is introduced:

$$\tau_{\mathrm{DP}} = \frac{\hbar}{\Delta E_{\mathrm{DP}}}. \tag{1}$$

where ΔE_{DP} measures, in gravitational terms, the self-potential difference of the states in superposition. If the mass density is $\mu(\mathbf{r})$ and the two states in superposition are displaced by a distance $\mathbf{d}$, ΔE_{DP} can be written:

$$\Delta E_{\mathrm{DP}}(\mathbf{d}) = -8\pi G \int \mathrm{d}\mathbf{r} \int \mathrm{d}\mathbf{r}' \frac{\mu(\mathbf{r})[\mu(\mathbf{r}'+\mathbf{d}) - \mu(\mathbf{r}')]}{|\mathbf{r}-\mathbf{r}'|}. \tag{2}$$

For microscopic and even partially for the molecular-scale, the so-called mesoscopic objects, the superposition is still possible, while, for the macroscopic system, they are almost instantaneously suppressed, recovering the reduction postulate. Each spontaneous collapse model, together with the collapsing spatial superposition, implies a Brownian-like diffusive motion acting on the system. If the system is electrically charged, this leads to the emission of a spontaneous radiation, and the details depend on the specific model [13,14]. In the case of the DP model, the expected photon emission rate $\mathrm{d}\Gamma/\mathrm{d}E$ per unit radiation energy E can be expressed as:

$$\frac{\mathrm{d}\Gamma}{\mathrm{d}E} = \frac{2}{3}\frac{Ge^2N^2N_a}{\pi^{3/2}\epsilon_0 c^3 R_0^3 E}. \tag{3}$$

where G, e, ϵ_0 and c are the gravitational constant, the electron charge, the vacuum permittivity and the speed of light, respectively. N_a represents the total number of atoms considered, while the factor N^2 accounts for the quadratic dependence on the atomic number, substantially increasing the effect. R_0 is the size of the particle's mass density, a parameter suggested by Penrose to be about the size of the wave function of the nucleus. R_0 can be, however, used as a free parameter of the model, as explained in Section 2.1.

The Continuous Spontaneous Localization (CSL) model is, together with the DP model, the most discussed dynamical reduction model in the literature [15,16]. In this model, the collapse does not take place as a result of the gravitational self-potential, but rather as interaction with a new, external noise field. The radiation rate in this case can be written as:

$$\frac{\mathrm{d}\Gamma}{\mathrm{d}E} = (N^2 + N)N_a \frac{\hbar\lambda}{4\pi^2\epsilon_0 m_0^2 r_C^2 c^3 E}. \tag{4}$$

where E is the energy of the radiation, and r_C and λ are the main model's parameter: the collapse spatial resolution and the strength of the noise, respectively. The factor $(N^2 + N)N_a$ incorporates the coherent emission from nuclei with N^2, and incoherent emission from electrons with N; m_0 is the reference nucleon mass. We have strongly constrained the available parameter space of both the DP and the CLS models, looking for the beyond-the-quantum-theory radiation, which is predicted to be emitted.

The quantum world can be investigated, as said above, also with a *top-down* approach, i.e., looking for physics beyond the SM. Quantum gravity theories, known as Non-Commutative Quantum Gravity (NCQG) models, can play such a role, modifying standard quantum mechanics principles. Non-commutative theories can be traced back to Heisenberg [17–19], developed later in the string theory [20] and loop quantum gravity theories [21]. In the NCQG theories, the Poincaré, κ–Poincaré and θ–Poincaré symmetries can be deformed (see [22–25] for the physical meaning of deformed Poincaré symmetries). The resulting deformation, strongly reduced at low energies, could cause a violation of the Pauli Exclusion Principle (PEP), which is related to the Spin Statistics theorem and the Lorentz/Poincaré symmetry. While a large class of these NCQG theories has been excluded by investigating the hadronic sector in nuclear transitions, in the leptonic sector, they have largely remained unconstrained.

The θ–Poincaré model predicts ([26] and references therein) that PEP is maximally violated close to the non-commutative scale Λ, and is highly suppressed at much smaller energies. The probability for electrons to perform PEP-violating transitions can be expressed as $\delta^2 = (E/\Lambda)^2$, where E is a combination of the characteristic energy scales of the transitions considered. In order to parametrize the emergence of PEP violation, a new phase, ϕ_{PEPV}, is introduced as a multiplicative factor to the standard transition probability W_0: $W_\theta = W_0 \cdot \phi_{\text{PEPV}}$. Explicitly factorizing the Λ dependence in the θ tensor, the phase can be expressed as:

$$\phi_{\text{PEPV}} = \delta^2 \simeq \frac{D}{2}\frac{E_N}{\Lambda}\frac{\Delta E}{\Lambda}, \text{ with } \theta_{0i} \neq 0 \qquad \phi_{\text{PEPV}} = \delta^2 \simeq \frac{C}{2}\frac{\bar{E}_1}{\Lambda}\frac{\bar{E}_2}{\Lambda}, \text{ with } \theta_{0i} = 0 \tag{5}$$

Here, $D/2$ and $C/2$ are factors close to one, E_N the nuclear energy, ΔE the atomic transition energy, and $\bar{E}_1$ and $\bar{E}_2$ the energy levels occupied by the initial and final electron states. θ_{0i} are the electric-like components of the θ tensor.

2. Experimental Results at LNGS

Under the Gran Sasso mountain in central Italy, at the INFN's national underground Laboratories (LNGS), the low radiation environment allows for pushing the limits of both the bottom-up and the top-down approaches. Protected by 1400 m of rock (3500 m of water equivalent), the LNGS hosts many experiments targeting beyond the SM physics, benefitting from a reduced cosmic radiation of about six orders of magnitude. The most relevant source of background is represented by the environmental radiation. We operate and take data with different apparatuses, which are presented in Section 2.1 for those dedicated to the collapse models, and in Section 2.2 for the one targeting the PEP violation.

2.1. Collapse Models

According to the DP and CSL collapse models, the random motion associated with the collapse in position causes the production of radiation, which is the detectable signal searched for in the Gran Sasso Laboratories. To this end, we employed a coaxial p-type lithium-doped high purity germanium detector with an active volume of 375 cm^3, shielded with electrolytic Copper and Lead, allocated within a steel housing in order to mitigate the impact of the residual environmental radiation [13], as schematically shown in Figure 1.

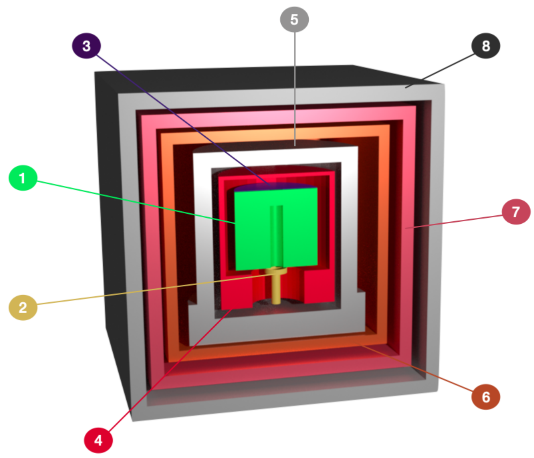

Figure 1. The details of the germanium detector used for collapse studies is shown in a schematic render. From inside out, (1) germanium crystal, (2) electric contact, (3) plastic insulator, (4,5,6) Copper cup, end-cup and block, (7) inner Copper shield and (8) Lead shield.

A Monte Carlo simulation was employed to describe the data acquired, which consists of the background radiation, originating mainly from residual cosmic rays penetrating the setup, and from radionuclide contamination. In order to determine whether the signal was present together with the background or not, a statistical analysis of the data was performed, parametrizing the signal hypothesis in terms of the model parameters and accounting for geometry, signal shape, and γ detection efficiency. No significant excess of events could be found beyond the expected ones, allowing for setting a lower limit on the R_0 parameter of the DP model [13]:

$$R_0 > 0.54 \times 10^{-10}\ \text{m}. \tag{6}$$

Since the size of the wave function in the germanium crystal is about $R_0 = 0.05 \times 10^{-10}$ m, this result effectively rules out the parameter-free version of the DP model [13].

The experimental apparatus searching for DP collapse model signal was also employed searching for signals of the CSL model. The spectrum is shown in Figure 2 (left), together with the background simulation. As for the DP model, no evidence of signal could be found with the statistical analysis, allowing for placing limits on the model [27], which are shown in Figure 2 (right) on the r_C–λ plane. The model is excluded from below by theoretical considerations (gray area), requiring that macroscopic objects collapse fast enough. Quantitatively, it is required that a single layered graphene disk of around 0.01 mm is localized in less than 10 ms. Gravitational wave detectors Auriga, Ligo and Lisa-Pathfinder can place a limit (red, blue and green lines on the plot, respectively), exploiting the collapse-induced noise on the detectors [28]. Finally, the spontaneous emission of radiation allows for closing the parameter space at lower r_C (purple and orange). The orange line is placed by the germanium detector, and the data described here improve by a factor of 13 the previous results. This limit was later improved by the MAJORANA DEMONSTRATOR [29] at the Sanford Underground Research Facility in Lead, South Dakota. The black markers represent the values proposed by Adler [30] and originating from the Ghirardi–Rimini–Weber (GRW) model [5].

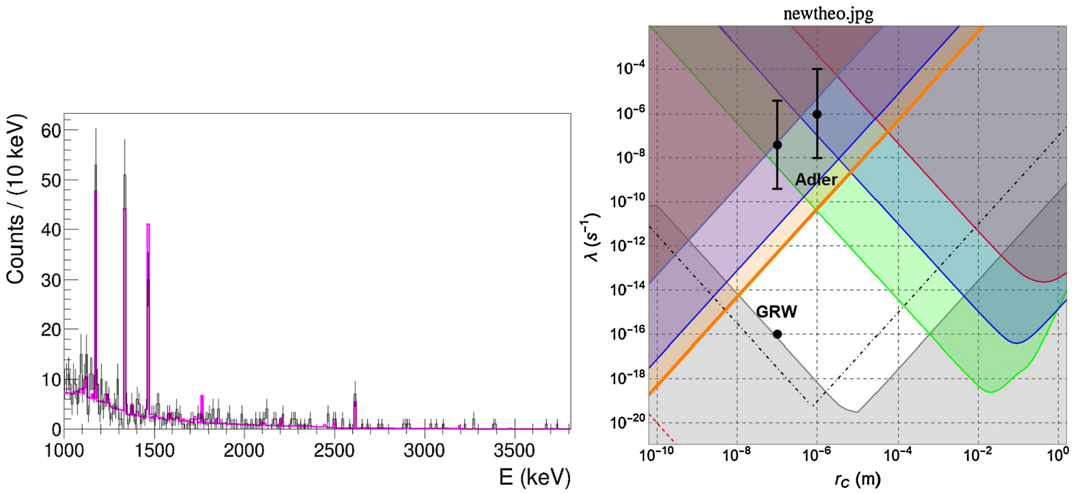

Figure 2. The results of the CSL model are shown: the data acquired (black line) and its simulation (purple line) are shown on the left. On the right, the r_C–λ parameter space and its bounds [27]. The limits from below are set by theoretical constraints, and the blue and orange lines are set by detection searching for spontaneous radiation. Red, blue and green lines are set by gravitational wave detectors Auriga, Ligo and Lisa-Pathfinder. The resulting limits from this measurement on the available parameter space of the model are an orange diagonal line in the r_C–λ plane. See text for details.

The bottom-up approach to testing quantum mechanics tries to reveal hints of possible new physics beyond the SM and the standard quantum theory, exploring its foundations. The century-old problem of the wave function collapse or the measurement problem has found renewed interest in the last few decades, and its solution could have a deep and broad impact on the understanding of the quantum world. With a state-of-the-art high purity germanium detector, in the cosmic silence of the LNGS, we have tested the predictions of the most important dynamical reduction models, setting strong limits which reduce even further the available parameter space.

2.2. Pauli Exclusion Principle Violations

The Pauli Exclusion Principle (PEP) is at the core of quantum mechanics since its original formulation in 1925 [31], based on few general assumptions, such as Lorentz and Poincaré and CPT symmetries, unitarity, causality and locality [32]. Beyond the SM, scenarios which incorporate a deformation of these basics principles could have an effect on the PEP. Theories such as classes of quantum gravity which entail a deformation of the commutativity of space-time, as in the Non-Commutative Quantum Gravity models, via modification of the Poincaré symmetry, could have an impact on the validity of the PEP even at low energies (see [21–23] and Section 2.4.2).

According to Messiah and Greenberg [33], it is not possible to observe PEP violating transitions without the introduction of new, external fermions: transitions between states with different symmetries are forbidden (MG superselection rule). Effectively, this result divides searches for PEP violation into two classes: those operating in *open* systems, meaning that the MG rule is enforced experimentally with an injection of new fermions, and those testing *closed* systems, meaning that there is no introduction of new particles and the MG constraint can be avoided considering a different class of PEP violation models. The NCQG theories κ– and θ–Poincaré evade the Messiah Greenberg constraint, therefore also allowing experimental tests in closed systems.

Attempts of formulating theoretical models which violate the statistics of identical particles were pioneered by Fermi [34], who discussed the implications of a—even tiny—non-identity of electrons. Ignatiev and Kuzmin elaborated a model consisting of a deformation of the standard Fermi oscillator [35]. In this approach, a three-level Fermi oscillator is considered, in which the additional level can be accessed with a probability

$\beta^2/2$. β is still currently used to represent the amplitude of a PEP violating transition in open systems, and $\beta^2/2$ is the violation probability.

Precision tests can put strong limits on the PEP violation probability ($\beta^2/2$ and δ^2), and, as a direct consequence, constrain the available classes of NCQG, as discussed in Section 2.2.

2.3. Open Systems: The VIP-2 Experiment

The VIP-2 experiment searches for a transition violating the PEP under the MG superselection rule, achieved via the introduction of external particles to test the exclusion principle. This is realized targeting forbidden $2p \rightarrow 1s$ transitions in Copper, as schematized in Figure 3, where new electrons introduced with a direct current can transit from the $2p$ state to the $1s$ state, which is already fully occupied. Since the additional electron provides an increased electromagnetic shielding, the X-rays emitted will have an energy slightly shifted downwards. Greenberg and Mohapatra [36] first indicated this experimental method, which was subsequently carried out by Ramberg and Snow [37].

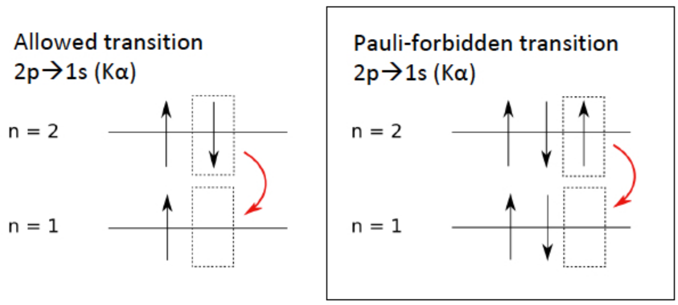

Figure 3. Schematic representation of the PEP allowed and forbidden $2p \rightarrow 1s$ transition: on the left, at $n = 1$, there is an unoccupied state; therefore, the transition can take place according to the PEP. On the right, the state is fully occupied, and the corresponding transition can take place only violating PEP.

The VIP-2 apparatus is shown as lateral and transverse views in Figure 4. It is an upgraded version of the predecessor VIP experiment. The goal of the VIP-2 experiment is to lower by two orders of magnitude the previous VIP limit, reaching $\beta^2/2 < 4 \times 10^{-31}$. To achieve this goal, the previously employed radiation detectors, Charge-Coupled Devices (CCDs), were replaced with state-of-the-art Silicon Drift Detectors (SDDs) which have a resolution of 190 eV (FWHM) at 8 keV, greater active area and quantum efficiency. The SDDs have been developed, tested and deployed in a collaboration within a Stefan Meyer Institute, Politecnico di Milano, Fondazione Bruno Kessler and INFN-LNF [38].

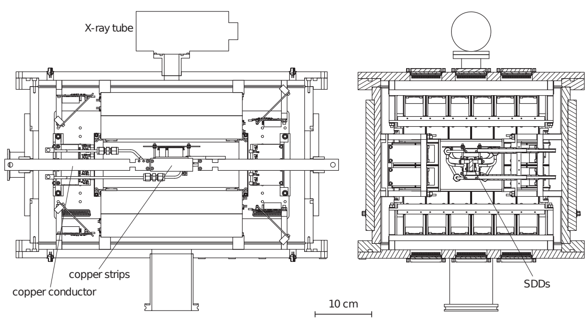

Figure 4. Later and transverse section of the VIP-2 setup at the LNGS, where a 180 A direct current is flown on the Copper strips (attached to the Copper conductor). Surrounding SDDs arrays visible on the transverse section are placed in front of the strips. The position of the X-ray tube is also indicated.

A pair of ultrapure electrolytic Copper strips of 71 mm × 20 mm × 25 μm are used as a target, and a direct current of up to 180 A is circulated between them. Four SDD arrays are placed, two in front of each strip, operated at a temperature of −90 °C. The target is kept at a stable temperature via a closer circuit chiller. A vacuum chamber houses the target, the SDDs and their front-end electronics, as well as a low activity Fe-55 source, used to provide an in situ calibration.

According to the MG superselection rule, new electrons arriving inside the target will test the PEP violation; if a forbidden transition takes place, a characteristic X-ray will be emitted at a lower energy with respect to the standard K_α.

Instead, when the current is not circulated, no PEP violating transition is expected, and the data are used as reference and stability control.

A first result of the VIP-2 setup is presented in Figure 5 from [39], which shows the spectra obtained in six months of data taking in 2020 with current on (cyan) and off (orange) together with the Copper and Nickel peaks. The analysis is carried out with a two-fold frequentist and Bayesian analysis to set at a 90% confidence level an upper limit on the number of signal events and therefore on the violation probability $\beta^2/2$. The statistical model which was employed is common for both spectra. The background is described with a first degree polynomial for the continuum component and with two Gaussian for the Copper and Nickel peaks. In the spectrum obtained with current, an additional Gaussian is added at 7.7 keV representing the PEP violating signal. A combined likelihood with external Gaussian constraint representing the energy scale and relative normalization of the two data-taking times is constructed. In the Bayesian description, the penalty terms are interpreted as priors. The prior for the number of signal events is assumed as a flat distribution.

The 90% CL upper limit on the signal yield was determined to consist of 54 events by using a modified frequentist CL_s method, and 52 events by using a Bayesian one. Following the original Ramberg and Snow experiment [37], the number of events can be translated into the PEP violation probability by considering the number of scattering of the injected electrons traveling along a straight line inside the target. The number of PEP violating X-rays is then expressed as

$$N_X = \beta^2/2 \cdot N_{int} \cdot N_{new} \cdot 1/10 \cdot \epsilon \tag{7}$$

where $N_{int} = D/\mu$ is the number of scatterings of the electrons (with D the target length and $\mu = 3.9 \times 10^{-6}$cm the electron scattering length in Copper), N_{new} the number of new electrons introduced with the current, $1/10$ is an estimate of the capture probability per scattering, and ϵ is the global geometrical and absorption efficiency of the X-ray inside the target, evaluated with a GEANT4 simulation. With these assumptions, the upper limits turn out:

$$\beta^2/2 \leq 8.6 \times 10^{-31} \text{ (Bayesian)}, \qquad \beta^2/2 \leq 8.9 \times 10^{-31} \text{ (CL}_s\text{)}. \tag{8}$$

A more effective model of the interactions of the electrons in the conduction band was developed (see details and further references in [39]), where the scatterings caused by interactions with phonons, lattice defects and impurities are replaced by *close encounters*, determined taking into account the Fermi velocity and the material density. In Copper, a conduction electron will have a close encounter every $\tau = 3.5 \times 10^{-17}$ s. The above relation (7) for the number of violating X-rays then becomes

$$N_X = \beta^2/2 \cdot N_{int} \cdot N_{new} \cdot \epsilon \tag{9}$$

With N_{int} now expressed as T/τ, where $T = l/v_D$ is the time the electron takes to travel through the distance l due to its drift velocity v_D. In this case, the exclusion limit on the PEP violation becomes [39]:

$$\beta^2/2 \leq 6.8 \times 10^{-43}\ \text{(Bayesian)}, \qquad \beta^2/2 \leq 7.1 \times 10^{-43}\ (\text{CL}_s). \tag{10}$$

The VIP-2 experiment has collected more than two years of data taking with the present configuration; with even more data being presently collected after a short technical stop. A publication of the entire available statistics is envisaged by the collaboration for the year 2023.

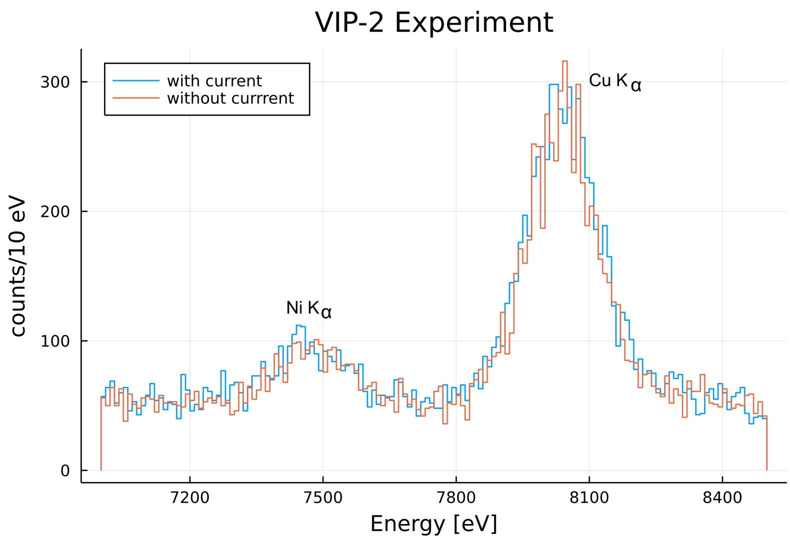

Figure 5. Energy calibrated spectra obtained by the VIP-2 experiment with full setup during six months of data taking in 2020 [39]. In cyan (orange), the spectrum obtained with current on (off) is presented in the region of interest 7–8.5 keV. The Copper and Nickel K_α lines are visible; the PEP violating signal is expected at around 7.7 keV, with a width similar to the standard one. The spectrum acquired without current is used as control and reference in the data analysis.

Future: VIP-3

The PEP surely plays a fundamental role in modern quantum physics. It is of great importance to continue with exhaustive tests, searching for possible violation across the entire periodic table, as outlined by L. B. Okun [40]. Within this framework, the VIP collaboration is planning an upgrade of the experimental setup, allowing for performing dedicated searches for PEP violation with a different Z target. To maximize the quantum efficiency even at higher Z (where it drops for present radiation detectors due to the higher penetration power of the more energetic X-rays), thicker 1 mm SDDs are in advance manufacturing stage by FBK. These SDDs will provide a factor two higher efficiency at 20 keV with respect to the 450 μm thick SDDs currently employed in the VIP-2 experiment, extending the experimental tests to Silver, Tin and Palladium. The new SDDs will be installed in a new apparatus, the VIP-3 experiment, which takes advantage of an improved vacuum chamber capable of housing twice the number of detectors, and of the possibility to inject a higher direct current up to 400 A.

2.4. VIP-Lead Closed System

The VIP-Lead closed system experiment uses a high-purity germanium detector to search for PEP violating processes in different scenarios, using low radioactivity Roman Lead. The MG superselection rule admits violating transitions only when new fermions are introduced in the system. However, this constraint can be partially relaxed if the target material has been recently cast from different original fragments. In this case, a search for *remnant* violation of the Pauli Exclusion principle can take place. On the other side, the

NCQG theories, such as κ- and θ–Poincaré, evade altogether the MG rule. In the following sections, an overview of the recent results obtained with the VIP-Lead closed system experiment in the remnant PEP violation scenario, and in the NCQG model, are presented.

The setup is schematically depicted in Figure 6 (left), showing the active germanium crystal and the surrounding cylinder of the Roman Lead target.

2.4.1. Remnant PEP Violation

In the Rahal and Campa formulation [41], if the symmetry violation is associated specifically to a 'wrong pair' of electrons, then PEP violation can be tested with conduction electrons. As discussed in [42], the time of close encounters of a free electron in the Fermi level in Lead is $\tau_{CE} = 2.5 \times 10^{-17}$s. Consequently, electrons in a target with an age on the geologic timescale would have interacted already with all the material atoms, leaving under MG no possibility of new PEP violating processes. Since the Roman Lead was melted and cast 16 years before the measurement, this still leaves a sizeable probability of remnant PEP violations.

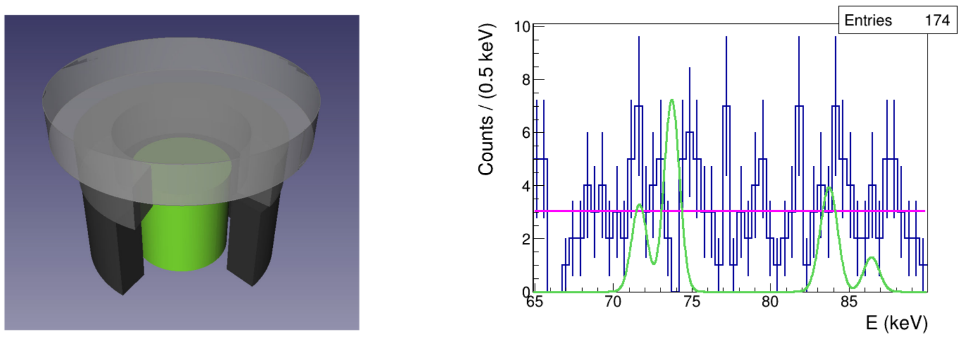

Figure 6. A schematic representation of the germanium detector used for closed systems tests of the PEP is shown on the left [42]. The green core is the active germanium crystal, and the surrounding black cylinder is the Roman Lead target. On the right, the spectrum acquired in the region of the standard and violating K_α transition in Lead is presented, looking for NCQG-induced PEP violating signals [26]. The green line represents the shape of the expected signal contribution in $\theta_{0i} \neq 0$, and the magenta line represents the fit on the background distribution.

No evidence for PEP was found in Lead; therefore, an upper limit on the $\beta^2/2$ probability was set [42]:

$$\beta^2/2 < 1.53 \times 10^{-43} \tag{11}$$

under the close encounters scenario for electrons.

2.4.2. NCQG-Induced PEP Violations

In the θ–Poincaré model, the scale where the PEP is maximally violated is the non-commutativity scale Λ. At lower energies, however, the PEP violating effects are maximally suppressed. With precision scrutiny of atomic transitions in the low radiation environment of the LNGS, it was possible to set strong limits on Λ for the different components of the θ tensor, in the leptonic sector. The PEP violating signal in Lead will again take place as an alteration of the K_α and K_β transitions energies at a lower energy with respect to the standard ones due to the additional energy shielding provided by the already-occupied 1s level. The rate predicted by the model can be expressed as:

$$\Gamma_{K_{\alpha 1}} = \frac{\delta^2(E_{K_{\alpha 1}})}{\tau_{K_{\alpha 1}}} \cdot \frac{BR_{K_{\alpha 1}}}{BR_{K_{\alpha 1}} + BR_{K_{\alpha 2}}} \cdot 6 \cdot N_{atom} \cdot \epsilon(E_{K_{\alpha 1}}). \tag{12}$$

where $E_{K_{\alpha 1}}$ represents the energy scale (different for the vanishing and non-vanishing θ_{0i} components of Equation (5)), $\tau_{K_{\alpha 1}}$, the lifetime of the standard 2p$\rightarrow$1s transition. The branching rations $BR_{K_{\alpha 1}}$ and $BR_{K_{\alpha 2}}$ take into account the different intensities of transitions originating from different j levels. N_{atom} is the number of atoms in the Lead sample, and the efficiency ϵ is derived with GEANT4 Monte Carlo simulation, taking into account the detection efficiency for the X-rays emitted inside the target. With a total integrated time of data taking $\Delta t \simeq 70$ days, the number of expected signal events is given by $\Gamma_{K_{\alpha 1}} \cdot \Delta t$, noting that the $\delta^2(E_{K_{\alpha 1}})$ PEP violation probability depends on $1/\Lambda^2$ in Equation (5). The spectrum in the region of interest of the Lead K_α lines is shown in Figure 6 (right), where the expected signal in the case of the non-vanishing electric-like components of θ is represented by a green line, and the fit of the background distribution in magenta. Performing a Bayesian analysis on the data, no evidence of excess over the expected number of background event was found, allowing setting limits on the non-commutativity scale. At a 90% confidence level, the upper limits on Λ are presented [26]:

$$\Lambda \geq 6.9 \times 10^{-2} \text{ Planck Scales (with } \theta_{0i} = 0), \tag{13}$$

$$\Lambda \geq 2.6 \times 10^{2} \text{ Planck Scales (with } \theta_{0i} \neq 0) \tag{14}$$

The vanishing electric-like component is therefore strongly constrained, while the non-vanishing one is excluded far above the Planck scale, providing the strongest experimental tests of the θ–Poincaré NCQG model in the leptonic sector by atomic transitions.

3. Conclusions

The very basis of Quantum Mechanics is being studied at the Gran Sasso National Laboratory by the VIP collaboration, from a bottom-up and top-down perspectives [43]. The former stems from the measurement problem and the wave function collapse, which have motivated the development of theories altering the standard quantum theory. Of these theories, the DP and CSL models have received significant attention, and can be experimentally tested. The VIP collaboration has searched for evidence of spontaneous radiation at the time of collapse which is expected in both models, excluding the parameterless formulation of the DP model, and tightly restricting the available parameter space of the CSL one [13,27]. The top-down perspective focuses on effects that new physics beyond the Standard Model could imply on phenomena at the quantum scale. Non-commutative Quantum Gravity theories postulate a modification of the space-time commutativity, intimately tied to CPT invariance, unitarity, causality and locality, and as a consequence a PEP violation. The VIP-2 detector is searching for PEP violation signals, in an open system setting, with a high intensity current injected in the Copper strip target in order to comply with the MG rule. The statistical analysis of half a year's worth of data demonstrates significant progress towards the experimental goals. Meanwhile, the collaboration is also concluding the design of the experimental upgrade, VIP-3, which will be equipped with a larger amount of SDDs and a higher direct current. The manufacture of 1 mm-thick SDDs, already at a final stage, will enable the progression of PEP violation searches to higher energy ranges. Finally, in closed systems, the MG can be relaxed for remnant PEP violation in recently cast low radioactivity Roman Lead, allowing as well to set strong limits on NCQG theories by exploiting high purity p-type germanium detectors. The non-commutative scale Λ of the θ–Poincaré theory is strongly constrained for the first time in the leptonic sector far above the Planck scale in the non-vanishing electric-like component of the θ tensor, and close to it in the vanishing case.

Author Contributions: Conceptualization, C.C.; Data curation, F.N.; Formal analysis, C.C. and K.P.; Funding acquisition, C.C. and J.M.; Investigation, F.N., A.A., A.B., M.B. (Massimiliano Bazzi), M.B. (Mario Bragadireanu), M.C., A.C., M.D., S.D., L.D.P., R.D.G., C.F., C.G., M.I., M.L., S.M., A.M., J.M., M.M., E.M., K.P., A.P., A.S., F.S. (Francesco Sgaramella), D.L.S., F.S. (Florin Sirghi), O.V.D., J.Z. and C.C.; Methodology, F.N. and K.P.; Project administration, C.C.; Resources, K.P. and C.C.; Software, F.N.; Supervision, K.P., F.N. and C.C.; Validation, F.N.; Visualization, F.N.; Writing—original draft, F.N.; Writing—review and editing, F.N., A.A., A.B., M.B. (Massimiliano Bazzi), M.B. (Mario Bragadireanu), M.C., A.C., M.D., S.D., L.D.P., R.D.G., C.F., C.G., M.I., M.L., S.M., A.M., J.M., M.M., E.M., K.P., A.P., A.S., F.S. (Francesco Sgaramella), D.L.S., F.S. (Florin Sirghi), O.V.D., J.Z. and C.C. All authors have read and agreed to the published version of the manuscript.

Funding: This publication was made possible through the support of Grant No. 62099 from the John Templeton Foundation. The opinions expressed in this publication are those of the authors and do not necessarily reflect the views of the John Templeton Foundation. We acknowledge support from the Foundational Questions Institute and Fetzer Franklin Fund, a donor advised fund of Silicon Valley Community Foundation (Grant No. FQXi- RFP-CPW-2008 and No. FQXi-MGB-2011), and from the H2020 FET TEQ (Grant No. 766900). Austrian Science Foundation (FWF) supports the VIP-2 project with the Grant No. P25529-N20,Projects No. P 30635-N36 and W1252-N27 (doctoral college particles and interactions). K. P. acknowledges support from the Centro Ricerche Enrico Fermi-Museo Storico della Fisica e Centro Studi e Ricerche "Enrico Fermi" (Open Problems in Quantum Mechanics project). A. A.'s work is supported by the Talent Scientific Research Program of College of Physics, Sichuan University, Grant No. 1082204112427 and the Fostering Program in Disciplines Possessing Novel Features for Natural Science of Sichuan University, Grant No. 2020SCUNL209 and 1000 Talent program of Sichuan province 2021. A.M. wishes to acknowledge support by the Shanghai Municipality, through the Grant No. KBH1512299, by Fudan University, through the Grant No. JJH1512105, the Natural Science Foundation of China, through the Grant No. 11875113, and by the Department of Physics at Fudan University, through the Grant No. IDH1512092/001. A.B. acknowledges financial support from the HE EIC Project QuCOM (Grant No. 101046973).

Informed Consent Statement: Not applicable.

Data Availability Statement: The data presented in this study are available on request from the corresponding author.

Acknowledgments: We thank the INFN Institute, for supporting the research presented in this article and, in particular, the Gran Sasso underground laboratory of INFN, INFN-LNGS, and its Director, Ezio Previtali, the LNGS staff, and the Low Radioactivity laboratory for the experimental activities dedicated to the search for spontaneous radiation. A.A. and A.M. would like to thank Rita Bernabei and Pierluigi Belli for useful discussions on this subject.

Conflicts of Interest: The authors declare no conflict of interest. The funding sponsors had no role in the design of the study; in the collection, analyses, or interpretation of data; in the writing of the manuscript, and in the decision to publish the results.

References

1. Schrödinger, E. Die gegenwärtige Situation in der Quantenphysik II. *Naturwissenschaften* **1935**, *23*, 823–828. [CrossRef]
2. Leggett, A.J. Macroscopic quantum systems and the quantum theory of measurement. *Prog. Theor. Phys. Suppl.* **1980**, *69*, 80–100. [CrossRef]
3. Weinberg, S. Precision tests of quantum mechanics. In *The Oskar Klein Memorial Lectures 1988–1999*; World Scientific: Singapore, 2014; pp. 61–68.
4. Bell, J.S.; Aspect, A. *Speakable and Unspeakable in Quantum Mechanics*; Cambridge University Press: Cambridge, UK, 2004. [CrossRef]
5. Ghirardi, G.C.; Rimini, A.; Weber, T. Unified dynamics for microscopic and macroscopic systems. *Phys. Rev. D* **1986**, *34*, 470. [CrossRef] [PubMed]
6. Adler, S.L. *Quantum Theory as an Emergent Phenomenon*; Cambridge University Press: Cambridge, UK, 2004. [CrossRef]
7. Weinberg, S. Collapse of the state vector. *Phys. Rev. A* **2012**, *85*, 062116. [CrossRef]
8. Penrose, R. On gravity's role in quantum state reduction. *Gen. Relativ. Gravit.* **1996**, *28*, 581–600. [CrossRef]
9. Penrose, R. On the gravitization of quantum mechanics 1: Quantum state reduction. *Found. Phys.* **2014**, *44*, 557–575. [CrossRef]
10. Howl, R.; Penrose, R.; Fuentes, I. Exploring the unification of quantum theory and general relativity with a Bose–Einstein condensate. *New J. Phys.* **2019**, *21*, 043047. [CrossRef]
11. Diósi, L. A universal master equation for the gravitational violation of quantum mechanics. *Phys. Lett. A* **1987**, *120*, 377–381. [CrossRef]
12. Diósi, L. Models for universal reduction of macroscopic quantum fluctuations. *Phys. Rev. A* **1989**, *40*, 1165. [CrossRef]
13. Donadi, S.; Piscicchia, K.; Curceanu, C.; Diósi, L.; Laubenstein, M.; Bassi, A. Underground test of gravity-related wave function collapse. *Nat. Phys.* **2020**, *17*, 74–78. [CrossRef]
14. Fu, Q. Spontaneous radiation of free electrons in a nonrelativistic collapse model. *Phys. Rev. A* **1997**, *56*, 1806–1811. [CrossRef]
15. Pearle, P. Combining stochastic dynamical state-vector reduction with spontaneous localization. *Phys. Rev. A* **1989**, *39*, 2277–2289. [CrossRef]

16. Ghirardi, G.C.; Pearle, P.; Rimini, A. Markov processes in Hilbert space and continuous spontaneous localization of systems of identical particles. *Phys. Rev. A* **1990**, *42*, 78–89. [CrossRef]
17. Jackiw, R. Physical instances of noncommuting coordinates. *Nucl. Phys.* **2002**, *108*, 30. [CrossRef]
18. Letter of Heisenberg to Peierls (1930). In *Wissenschaftlicher Briefwechsel mit Bohr, Einstein, Heisenberg u.a. Band II: 1930–1939. p.15/Scientific Correspondence with Bohr, Einstein, Heisenberg a.o. Volume II: 1930–1939. p.15*; von Meyenn, K., Ed.; Springer: Berlin/Heidelberg, Germany, 1985. [CrossRef]
19. Letter of Pauli to Oppenheimer (1946). In *Wissenschaftlicher Briefwechsel mit Bohr, Einstein, Heisenberg u.a. Band III: 1940–1949. p. 380/Scientific Correspondence with Bohr, Einstein, Heisenberg, a.o., Volume III: 1940–1949. p. 380*; von Meyenn, K., Ed.; Springer: Berlin/Heidelberg, Germany. [CrossRef]
20. Seiberg, N.; Witten, E. String theory and noncommutative geometry. *J. High Energy Phys.* **1999**, *1999*, 032. [CrossRef]
21. Brahma, S.; Ronco, M.; Amelino-Camelia, G.; Marcianò, A. Linking loop quantum gravity quantization ambiguities with phenomenology. *Phys. Rev. D* **2017**, *95*, 044005. [CrossRef]
22. Arzano, M.; Kowalski-Glikman, J. Deformed discrete symmetries. *Phys. Lett. B* **2016**, *760*, 69–73. [CrossRef]
23. Addazi, A.; Marcianò, A. A modern guide to θ–Poincaré. *Int. J. Mod. Phys. A* **2020**, *35*, 2042003. [CrossRef]
24. Amelino-Camelia, G.; Freidel, L.; Kowalski-Glikman, J.; Smolin, L. Principle of relative locality. *Phys. Rev. D* **2011**, *84*, 084010. [CrossRef]
25. Amelino-Camelia, G. Special treatment. *Nature* **2002**, *418*, 34–35. [CrossRef]
26. Piscicchia, K.; Addazi, A.; Marcianò, A.; Bazzi, M.; Cargnelli, M.; Clozza, A.; De Paolis, L.; Del Grande, R.; Guaraldo, C.; Iliescu, M.A.; et al. Strongest Atomic Physics Bounds on Noncommutative Quantum Gravity Models. *Phys. Rev. Lett.* **2022**, *129*, 131301. [CrossRef] [PubMed]
27. Donadi, S.; Piscicchia, K.; Grande, R.D.; Curceanu, C.; Laubenstein, M.; Bassi, A. Novel CSL bounds from the noise-induced radiation emission from atoms. *Eur. Phys. J. C* **2021**, *81*. [CrossRef]
28. Carlesso, M.; Bassi, A.; Falferi, P.; Vinante, A. Experimental bounds on collapse models from gravitational wave detectors. *Phys. Rev. D* **2016**, *94*. [CrossRef]
29. Arnquist, I.J.; Avignone, F.T.; Barabash, A.S.; Barton, C.J.; Bhimani, K.H.; Blalock, E.; Bos, B.; Busch, M.; Buuck, M.; Caldwell, T.S.; et al. Search for Spontaneous Radiation from Wave Function Collapse in the Majorana Demonstrator. *Phys. Rev. Lett.* **2022**, *129*, 080401. [CrossRef] [PubMed]
30. Adler, S. Lower and upper bounds on CSL parameters from latent image formation and IGM heating. *J. Phys. A* **2007**, *40*, 2935. Correction in *J. Phys. A Math. Theor.* **2007**, *40*, 13501. [CrossRef]
31. Pauli, W. Über den Zusammenhang des Abschlusses der Elektronengruppen im Atom mit der Komplexstruktur der Spektren. *Z. Für Phys.* **1925**, *31*, 765. [CrossRef]
32. Lüders, G.; Zumino, B. Connection between Spin and Statistics. *Phys. Rev.* **1958**, *110*, 1450–1453. [CrossRef]
33. Messiah, A.M.L.; Greenberg, O.W. Symmetrization Postulate and Its Experimental Foundation. *Phys. Rev.* **1964**, *136*, B248–B267. [CrossRef]
34. Fermi, E. Le Ultime Particelle Costitutive Della Materia. *Scientia* **1934**, *28*, 21.
35. Ignatiev, A.Y.; Kuzmin, V. Search for slight violation of the Pauli principle. *JETP Lett.* **1987**, *47*, 6–8.
36. Greenberg, O.W.; Mohapatra, R.N. Local Quantum Field Theory of Possible Violation of the Pauli Principle. *Phys. Rev. Lett.* **1987**, *59*, 2507–2510. [CrossRef]
37. Ramberg, E.; Snow, G.A. Experimental limit on a small violation of the Pauli principle. *Phys. Lett. B* **1990**, *238*, 438–441. [CrossRef]
38. Quaglia, R.; Bombelli, L.; Busca, P.; Fiorini, C.; Occhipinti, M.; Giacomini, G.; Ficorella, F.; Picciotto, A.; Piemonte, C. Silicon Drift Detectors and CUBE Preamplifiers for High-Resolution X-ray Spectroscopy. *IEEE Trans. Nucl. Sci.* **2015**, *62*, 221–227. [CrossRef]
39. Napolitano, F.; Bartalucci, S.; Bertolucci, S.; Bazzi, M.; Bragadireanu, M.; Capoccia, C.; Cargnelli, M.; Clozza, A.; De Paolis, L.; Del Grande, R.; et al. Testing the Pauli Exclusion Principle with the VIP-2 Experiment. *Symmetry* **2022**, *14*, 893. [CrossRef]
40. Okun, L.B. On the Possibility of Pauli Principle Violation in Atoms. *JETP Lett.* **1987**, *46*, 529–532.
41. Rahal, V.; Campa, A. Thermodynamical implications of a violation of the Pauli principle. *Phys. Rev. A* **1988**, *38*, 3728–3731. [CrossRef]
42. Piscicchia, K.; Milotti, E.; Amirkhani, A.; Bartalucci, S.; Bertolucci, S.; Bazzi, M.; Bragadireanu, M.; Cargnelli, M.; Clozza, A.; Egger, J.P.; et al. Search for a remnant violation of the Pauli exclusion principle in a Roman lead target. *Eur. Phys. J. C Part. Fields* **2020**, *80*, 508. [CrossRef]
43. Curceanu, C.; Napolitano, F.; Bartalucci, S.; Bertolucci, S.; Bazzi, M.; bragadireanu, M.; Capoccia, C.; Cargnelli, M.; Clozza, A.; De Paolis, L.; et al. Underground tests of Quantum Mechanics at Gran Sasso. In Proceedings of the 7th Symposium on Prospects in the Physics of Discrete Symmetries, Bergen, Norway, 29 November–3 December 2022; p. 5. [CrossRef]